Ashdin Publishing
Journal of Drug and Alcohol Research
Vol. 1 (2012), Article ID 235607, 9 pages
doi:10.4303/jdar/235607

Research Article

Assessment of Potential Neuronal Toxicity of Inhaled Anesthetics in the Developing Nonhuman Primate

Fang Liu, Xuan Zhang, Tucker A. Patterson, Shuliang Liu, Syed F. Ali, Merle G. Paule, William Slikker Jr., and Cheng Wang

Division of Neurotoxicology, National Center for Toxicological Research/U.S. Food and Drug Administration, Jefferson, AR 72079, USA
Address correspondence to Cheng Wang, cheng.wang@fda.hhs.gov

Received 27 June 2012; Accepted 12 July 2012

Abstract Anesthetics have been used for years in pediatric patients without clinical evidence of adverse central nervous system (CNS) sequelae. In the current study, postnatal day (PND) 5–6 rhesus monkeys were exposed to nitrous oxide (N_2O; 70%) alone, isoflurane (ISO; 1.0%) alone, or N_2O plus ISO for 8 h. Six hours after completion of anesthetic administration, neuronal toxicity was examined using histochemical and molecular imaging approaches. Histochemical data demonstrated that exposure of the developing monkey to the inhaled anesthetic combination for 8 h results in significantly enhanced neuronal cell death in frontal cortex, temporal gyrus, and hippocampus. Imaging techniques also demonstrated that such anesthetic exposure causes significant neuronal damage in cortical brain regions as indicated by an elevated binding of the specific peripheral benzodiazepine receptor radiotracer [^{18}F]-N-(2-(2-fluoroethoxy)benzyl)-N-(4-phenoxypyridin-3-yl) acetamide ([^{18}F]-FEPPA), a marker of activated microglia or inflammatory responses. No significant neurotoxic effects were observed in monkeys treated with N_2O alone, ISO alone, or in monkeys treated with the anesthetic combination for only 3 h. These data suggest that prolonged exposures to inhaled anesthetics in the developing rhesus monkey can result in significant neuronal damage.

Keywords inhaled anesthetics; developmental neurotoxicity; nonhuman primate

1 Introduction

Advances in pediatric and obstetric medicine have resulted in an increase in the complexity, duration, and number of anesthetic procedures. To minimize risks, it is necessary to understand the effects of anesthetics on the developing nervous system.

Most of the currently used general anesthetics have either N-methyl-D-aspartate (NMDA) receptor-blocking or gamma-aminobutyric acid type A (GABAA) receptor-activating properties. Nitrous oxide (N_2O), an NMDA receptor antagonist, and isoflurane (ISO), which acts on multiple receptors including postsynaptic GABA receptors, are probably the most widely used inhaled anesthetics being used alone or as part of a mixed anesthetic regimen (N_2O + ISO). Recent findings indicate that chemicals that act by either of these mechanisms can induce widespread neuronal apoptosis in the immature rat brain when administered during synaptogenesis [6,9,10,32,33]. It has also been reported that exposure of the developing brain to a clinically relevant cocktail of anesthetics that have both NMDA antagonist and GABA mimetic properties resulted in an extensive pattern of neuroapoptosis and subsequent cognitive deficits in rodents [13,38].

While it is clear that anesthetics cause neuronal cell death in the rodent model when given at significant doses during the brain growth-spurt period [10,30], it is not yet known to what degree similar phenomena also occur in primates. In order to determine if inhaled anesthetic-induced neurodegeneration in the developing rat has clinical relevance, nitrous oxide and isoflurane should be examined in a nonhuman primate model that more closely mimics the developing pediatric population [7,31]. The similarity of the physiology, pharmacology, metabolism, and reproductive system of the nonhuman primate to those of the human, especially during pregnancy, makes the monkey an exceptionally good model for use in detecting potential neurodegenerative effects of general anesthetics.

MicroPET technologies offer unique opportunities for imaging small animal models. It is an imaging modality applicable at the molecular level that can provide valuable insights into biochemical, physiological, pathological, and pharmacological processes in vivo [5,15,17,23]. One of the most important purposes of this study is to employ microPET imaging approaches in addressing the problem of developmental neurotoxicity produced by inhaled anesthetic agents. The utilization of imaging approaches can provide a framework on which information can be arranged in the form of a biological model to be used as a tool in dissecting out mechanisms underlying toxicological phenomena.

2 Materials and methods

2.1 Animals

All animal procedures were approved by the Institutional Animal Care and Use Committee (IACUC) at the National Center for Toxicological Research (NCTR) and conducted in full accordance with the Public Health Service (PHS) Policy on Humane Care and Use of Laboratory Animals.

All monkeys were born and housed at the FDA's National Center for Toxicological Research nonhuman primate research facility. Animal procedures were designed to minimize the number of animals required and any pain or distress associated with the experimental procedures.

A total of twenty-four (PND 5 or 6, 460–500 g) rhesus monkeys (*Macaca mulatta*) were utilized. Seven male and seventeen female monkeys were randomly assigned to six experimental groups and treated for 8 h as follows: (1) nitrous oxide (70%) alone ($n = 3$; 1 male, 2 females), (2) isoflurane (1.0%) alone ($n = 3$; 3 females), (3) 70% nitrous oxide + 1.0% isoflurane ($n = 5$; 1 male, 4 females), (4) control ($n = 5$; 2 males, 3 females), (5) 70% nitrous oxide + 1.0% isoflurane (for microPET scanning) ($n = 4$, 1 male, 3 females), and (6) control (for microPET scanning) ($n = 4$, 2 males, 2 females) groups. Animals from the first four groups were utilized for histopathological workup and animals from the last two groups were utilized for microPET imaging. Immediately prior to the initiation of anesthesia or sequestration, the infant monkeys were separated from their anesthetized mothers, removed from their home cage, and hand carried to a procedure room.

2.2 Anesthesia treatment

N_2O and oxygen were delivered using a calibrated anesthesia machine with blender (Bird Corporation, Palm Springs, CA, USA). Isoflurane (ISO) was delivered using an agent-specific vaporizer (E-Z Anesthesia, Palmer, PA, USA) attached to the anesthesia machine. To administer a specific concentration of N_2O/oxygen, ISO/oxygen, and N_2O/oxygen/ISO in a highly controlled environment, an anesthesia chamber was used. Monkeys were kept in this chamber with a circulating water heating pad to maintain body temperature at approximately 37 °C throughout the experiment. Stable gas and volatile anesthetic concentrations in the exposure chamber were obtained within 5 min of the start of the exposure. For controls, room air was used in the place of the inhaled anesthetics. For the anesthetic groups N_2O was administered at a concentration of 70% in oxygen for 8 h. ISO was delivered at 1% in oxygen. For the monkeys given the anesthetic mixture, N_2O, oxygen, and ISO were provided at approximately 70, 29, and 1%, respectively. A relief valve on the anesthesia chamber allowed a continuous escape of gases to avoid accumulation of carbon dioxide and waste gases were scavenged using an attached canister containing activated charcoal.

Throughout the exposures, dextrose (5%) was administered by a stomach tube (5 mL) every 2 h to both treated and control monkeys to maintain blood glucose levels. Glycopyrrolate (0.01 mg/kg, American Reagent, Shirley, NY, USA) was administered intramuscularly prior to anesthesia to both treated and control monkeys to reduce airway secretions. For the histochemical studies, animals were sacrificed 6 h after the end of the anesthesia using a dose of ketamine (20 mg/kg; IM), followed by transaortic perfusion with 0.9% saline and 4% paraformaldehyde in 0.1 M phosphate buffer. For the microPET studies, the first scan of each monkey brain was taken one day (24 h) after the anesthetic exposure on PND 6 or 7.

2.3 Physiological measurements

The procedures followed for the maintenance and monitoring of experimental subjects during anesthesia have been detailed in earlier publications [8,26]. Briefly, pulse oximetry (N-395 Pulse Oximeter, Nellcor, Pleasanton, CA, USA), capnography (Tidal Wave Hand-held Capnograph, Respironics, Murrysville, PA, USA), non-invasive sphygmomanometry (Critikon Dynamap Vital Signs Monitor, GE Healthcare, Waukesha, WI, USA), and a rectal temperature probe were used to monitor physiological conditions. Heart and respiratory rates, oxygen saturation of hemoglobin, expired CO_2 concentrations, and rectal temperatures were recorded every hour and systolic, diastolic, and mean arterial blood pressures were recorded every 2 h. Blood (0.25 mL) was collected at 1- to 2-h intervals for the measurement of plasma glucose (Ascensia Elite XL Blood Glucose Meter, Bayer Diagnostics, Tarrytown, NY, USA) and venous blood gases (Rapidlab, East Walpole, MA, USA).

2.4 Histopathology

2.4.1 Degeneration-selective silver staining

Coronal sections (40 μm) were cut through the whole brain using a freezing, sliding microtome and then rinsed in distilled water and processed for silver stain [18]. Briefly, sections were processed in a plastic staining basket with 24 wells and a vinyl mesh bottom. Sections were rinsed and pre-incubated in a pre-treating solution (9% NaOH + 1.2% NH_4NO_3) for 10 min. Sections were incubated in impregnating solution (9% NaOH + 16% NH_4NO_3 + 50% $AgNO_3$) for 10 min then rinsed in washing solution (1.2% NH_4NO_3 + 0.05% $C_6H_8O_7$). The sections were then processed in developing solution (0.05% $C_6H_8O_7$ + 1.2% NH_4NO_3) for 1 min, bleached with 0.5% acetic acid for 10 min, and mounted onto slides. Finally, the slides were air dried, placed in xylene, and cover-slipped with permount medium.

2.4.2 Anti-cleaved caspase-3 rabbit polyclonal antibody immunohistochemistry

Sections (40 μm) adjacent to those used for the silver stain were rinsed in 0.1 M potassium phosphate buffer (PPB) and processed for immunohistochemistry using a modification of a previously described procedure [27]. Briefly, sections were first washed in PPB (3×10 min) and in 0.3% hydrogen peroxide in PPB for 30 min at room temperature. Then the sections were incubated with the primary antibody at 4 °C overnight. A rabbit polyclonal antibody that detects human and mouse cleaved caspase-3 (1:500; Trevigen, Gaithersburg, MD, USA), one of the key effectors of apoptosis, was used.

Bound antibodies were visualized using biotin-conjugated goat anti-rabbit secondary antibodies (diluted 1:100) at room temperature for 1 h. After washing in PPB, sections were immersed in peroxidase conjugated streptavidin (1:200) for 1 h at room temperature then in 3,3-diaminobenzidine tetrahydrochloride (Sigma, St. Louis, MO, USA), placed on slides and examined with a Nikon microscope.

In order to measure the density and distribution of anti-cleaved caspase-3 rabbit polyclonal antibody (caspase-3)-, Fluoro-Jade C- and silver-stain positive neural cells, the following procedures were performed. After carefully reviewing the 40-μm coronal sections (for the whole monkey brain including cortical brain regions, hippocampus, thalamus, striatum, amygdala, and cerebellum), it was determined that the effects of inhaled anesthetic exposure (N_2O + ISO; for 8 h) on these monkey brains were primarily restricted to the cortical brain regions, especially the frontal cortex, temporal gyrus and hippocampus [22]. Adjacent pre- and post-serial sections were selected for morphological and statistical measurements.

2.4.3 Fluoro-Jade C staining

Coronal sections (40 μm) adjacent to those used for silver staining were rinsed in PPB and also processed for Fluoro-Jade C staining using a modification of a previously described procedure [25]. Prior to staining, sections were mounted onto positively charged slides. Slides were first immersed in a basic alcohol solution consisting of 1% NaOH in 80% ethanol for 5 min, followed by a wash for 2 min in 70% ethanol and distilled water, and incubated in 0.06% potassium permanganate solution for 10 min. Slides were then transferred for 25 min to a 0.0001% solution of Fluoro-Jade C (Histo-Chem Inc., Jefferson, AR, USA) dissolved in 0.1% acetic acid. The proper dilution was accomplished by first making a 0.01% stock solution of the dye in distilled water and then adding 1 mL of the stock solution to 99 mL of 0.1% acetic acid. The slides were rinsed through three changes of distilled water for 1 min per change. The air-dried slides were cleared in xylene and then cover-slipped with DPX non-fluorescent mounting media (Sigma, St. Louis, MO, USA).

2.4.4 Quantitative analysis

To determine the number of damaged neural cells, a PC-based image analysis system (MCID, Imaging Research, Inc., St. Catherines, ON, Canada) interfaced with an Olympus Vanox microscope by way of a solid state video camera was used. Unbiased sampling for each monkey was performed by randomly selecting five viewing fields (10X)/section from six serial frontal cortical, temporal gyrus, and hippocampal sections collected from the same location from each monkey. These viewing fields were counted by a trained expert and confirmed by another rater were blind to the treatment. The threshold was determined interactively by a consensus of two trained observers and then held constant for all viewing fields [24].

2.4.5 MicroPET

A commercial high-resolution small-animal PET scanner (Focus 220, Siemens Preclinical Solution, Knoxville, TN, USA) was used to quantitatively acquire images of the monkey brain. The scanner has 96 lutetium oxyortho-silicate detectors and provides a transaxial resolution of 1.35 mm full-width at half-maximum. Data were collected in a $128 \times 128 \times 95$ matrix with a pixel width of 0.475 mm and a slice thickness of 0.815 mm.

The first microPET scan of each monkey brain occurred on the day following the experimental exposures. Follow-up microPET scans occurred approximately one week, three weeks, and 6 months following the anesthetic exposure. For collection of the microPET images, animals were positioned on a modified external bed controlled by the microPET unit. Throughout microPET imaging sessions, monkeys were anesthetized with 1.5% isoflurane gas alone delivered through a custom face mask. An electronic heating pad was used to maintain body temperature at approximately 37 °C. For each imaging session [^{18}F]-FEPPA (56 MBq) was injected into the lateral saphenous vein of each anesthetized animal. Immediately following the injection, a set of serial microPET images was collected to assess the brain concentration of [^{18}F]-FEPPA for 2 h (24 frames, 5 min each).

2.4.6 Imaging data analysis

Medical image analysis software ASIPro (Concorde Microsystems, Inc, Knoxville, TN, USA) was used for the molecular imaging data and statistical analyses. Regions of Interest (ROIs) were outlined and measured using tools provided by ASIPro. Radioactivity in different brain areas was also quantified using this software. All images were displayed using the same color scale. Tracer accumulations in the ROIs were converted to Standard Uptake Values [SUVs = average concentration of radioactivity in the ROI

Table 1: Physiological parameters for infant monkeys exposed to inhaled anesthetics (adapted from Zou et al. [36]).

	PND 5/6 monkeys			
	Control	ISO	N_2O	ISO+N_2O
Respiratory rate (breaths/min)	63 ± 4.8	66 ± 3.1	73 ± 5.5	60 ± 12.5
Heart rate (beats/min)	219 ± 24.1	186 ± 44.6	213 ± 24.7	188 ± 28.5
O_2 saturation (%)	95 ± 2.5	91 ± 1.8	95 ± 3.7	94 ± 0.9
Temperature (°C)	36.6 ± 0.5	34.8 ± 1.4	36.3 ± 0.6	34.5 ± 1.8
Systolic blood pressure	77 ± 9.5	75 ± 4.5	79 ± 11.7	86 ± 12.1
Diastolic blood pressure	49 ± 4.4	43 ± 3.6	58 ± 10.5	59 ± 13.9
Glucose (mg/dl)	68 ± 13.5	72 ± 13.7	85 ± 17.4	80 ± 10.1
Venous pCO_2	45 ± 9.2	60 ± 1.0	49 ± 6.9	54 ± 10.6
Venous pO_2	26 ± 15.0	28 ± 4.2	27 ± 5.5	28 ± 4.7
Venous pH	7.3 ± 0.1	7.3 ± 0.02	7.2 ± 0.04	7.3 ± 0.08
Venous O_2 saturation	33 ± 10.7	52 ± 10.7	30 ± 5.1	45 ± 9.6

(mCi/mL) × body weight in grams/injected dose (mCi)]. The SUVs for the ROIs were compared between control and treatment groups at a variety of time points using RM ANOVA. All values are presented as means ±S.E.M. A P-value less than 0.05 was considered statistically significant.

3 Results

3.1 Physiologic responses to anesthetic exposure

All monkeys tolerated the procedures well and recovered from the anesthesia or sequestration (time in the exposure chamber) readily and were returned to and accepted by their mothers without incident. During the exposure to the combination of 70% N_2O plus 1% ISO, physiological values such as body temperature, blood glucose, and O_2 saturation levels remained within normal ranges for both control and anesthetic-treated monkeys. Heart rate was slightly decreased in the ISO or N_2O alone and N_2O + ISO-treated monkeys, compared to controls. Consistent with differences in heart rate, venous pCO_2 was a little higher in anesthetic (ISO or N_2O alone and N_2O + ISO)-treated monkeys than in controls. Body temperature, blood pressure, and venous pH did not vary significantly between groups. Oxygen saturation of hemoglobin measured by pulse oximetry was 91–95% for all groups. Table 1 summarizes the physiological variables for the control and inhaled anesthetic-treated groups. None of these parameters were significantly different among groups as determined by one-way ANOVA.

3.2 Histochemical evidence of prolonged inhaled anesthetic-induced neurotoxicity

Brains from the monkeys treated with the inhaled anesthetic combination [N_2O (70%) + ISO (1.0%)] for 8 h showed a marked increase in the number of silver stained neurons compared to those from the control monkeys (Figure 1). Silver-positive neuronal cells were prominent in the neocortical areas, especially in layers II and III of the frontal cortex (Figure 1(B)), hippocampus (Figure 1(D)) and temporal gyrus (Figure 1(F)) compared with their controls (Figures 1(A), 1(C), and 1(E)). No significant effects were detected when the monkeys were treated with

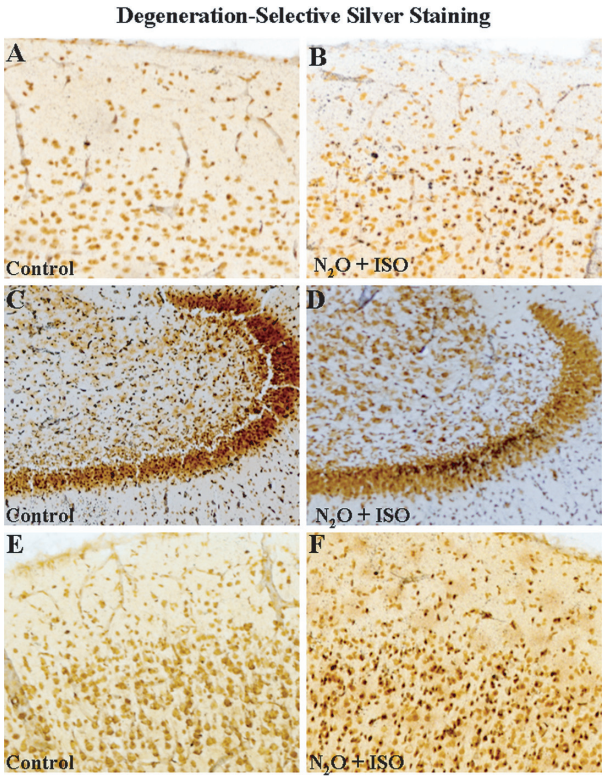

Figure 1: Effects of exposure to the inhaled anesthetic combination [70% N_2O + 1% ISO] on silver-impregnated neuronal profiles. Prolonged inhaled anesthetic exposure caused enhanced neuronal damage as indicated by an increase in the density of silver grains in areas of the frontal cortex (Figure 1(B)), hippocampus (Figure 1(D)) and temporal gyrus (Figure 1(F)) compared with their controls (Figures 1(A), 1(C), and 1(E)). At least three monkeys per group were randomly assigned to treatment and control groups.

Table 2: Statistical analyses for the histochemical endpoints.

	Frontal cortex		Hippocampus		Temporal gyrus	
	Control	Treated	Control	Treated	Control	Treated
Silver	17.8 ± 24.6	$132.2 \pm 152.5^*$	25.9 ± 15.1	$369.6 \pm 323.3^*$	15.8 ± 1.1	$63.9 \pm 38.0^*$
Caspase-3	5.7 ± 1.0	$24.4 \pm 10.3^*$	8.7 ± 1.6	$13.8 \pm 2.5^*$	3.5 ± 0.8	$9.9 \pm 4.4^*$
Fluoro-Jade C	4.1 ± 1.7	$16.4 \pm 3.6^*$	4.8 ± 0.6	$20.2 \pm 5.0^*$	4.4 ± 04	$172.4 \pm 32^*$

Values are means $\pm$ SD (numbers per section) from at least 3 monkeys/group. For silver, the numbers indicate grain counts; for caspase-3 and Fluoro-Jade C, the numbers indicate cell counts.

*It indicates a significant difference ($P < .05$) between control and treated monkeys.

the same anesthetic combination for 3 h; and no significant neurotoxicity was observed in the animals treated with either N_2O (70%) or ISO (1.0%) alone (data not shown).

Consistent with the silver stain profiles, Table 2 shows that the exposure to the anesthetic combination for 8 h produced an elevated neuronal cell death as indicated by other histochemical approaches including caspase-3- and Fluoro-Jade C-staining in the cortical brain regions. Only a few silver-, caspase-3- and Fluoro-Jade C-positive cells were observed in the controls; however, numerous silver-, caspase-3- and Fluoro-Jade C-positive neuronal profiles, indicative of enhanced neuronal damage, were observed in animals exposed to the anesthetic combination (Table 2).

3.3 Molecular imaging evidence of prolonged inhaled anesthetic-induced neurotoxicity

On PND 6/7, one day after the monkeys were treated with the anesthetic mixture, [^{18}F]-FEPPA (56 MBq) was injected into the lateral saphenous vein and dynamic microPET images were immediately obtained over the next 2 h. Figure 2 shows a set of representative microPET images, displayed in coronal, transverse and sagittal planes and highlighting [^{18}F]-FEPPA brain concentrations in a monkey treated with the anesthetic mixture. The accumulation of [^{18}F]-FEPPA was significantly increased in cortical areas including the temporal lobe.

The first microPET scans were taken on PND 6 or 7, one day (24 h) after the end of anesthetic exposure, and follow-up scans were obtained for each monkey on PNDs 14 and 30 and at 6 months of age. For each microPET scan, images were obtained for 2 h following the injection of [^{18}F]-FEPPA. Accumulations of radioactivity in the ROIs were converted to SUVs. [^{18}F]-FEPPA was observed in the ROIs in both control and treated animals demonstrating that it was distrubted to these brain areas. The first microPET scans (24 h after anesthetic treatment) are shown in Figure 3(A), where it can be seen that the accumulation of [^{18}F]-FEPPA was increased in cortical areas such as the temporal lobe, with significant differences being observed at some time points. The uptake of [^{18}F]-FEPPA in the frontal lobe of treated animals was not significantly increased in treated animals even though the SUVs at most time points were higher than in controls.

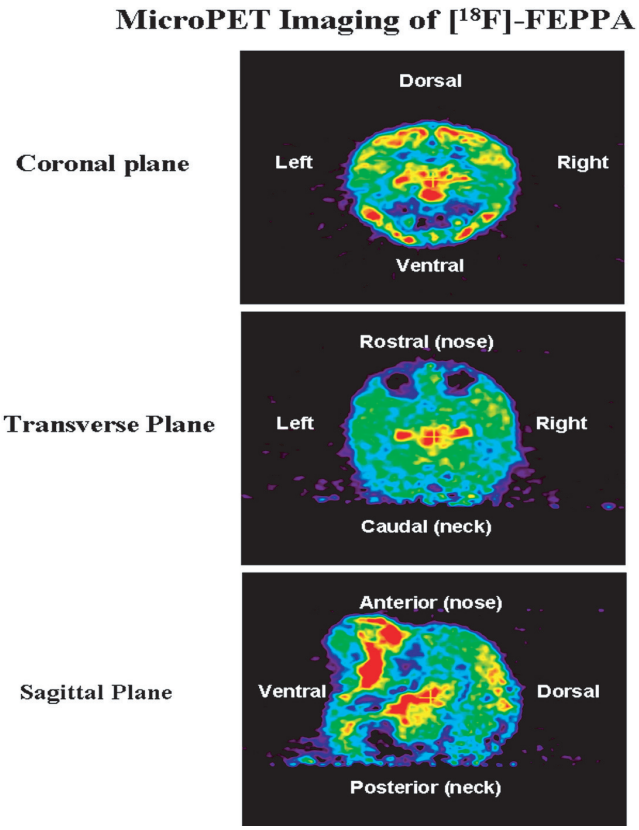

Figure 2: MicroPET images shown in coronal, sagittal and transverse planes highlighting [^{18}F]-FEPPA brain concentrations in a monkey one day (24 h) after an 8-h exposure to a combination of 70% N_2O + 1% ISO. The 2-h microPET scan began immediately after [^{18}F]-FEPPA administration.

On PND 14, approximately one week after the anesthetic exposure, SUVs in temporal cortical areas were higher (but not significantly so) in the treated animals than in the controls at all time points, demonstrating a continued increased uptake and retention of [^{18}F]-FEPPA in treated subjects (Figure 3(B)). Significant differences in SUVs were, however, observed only in the frontal cortical area.

On PND 30, about 3 weeks after anesthetic exposure, the uptake of [^{18}F]-FEPPA in the treated monkeys was higher than that in the controls at most of the time points, although

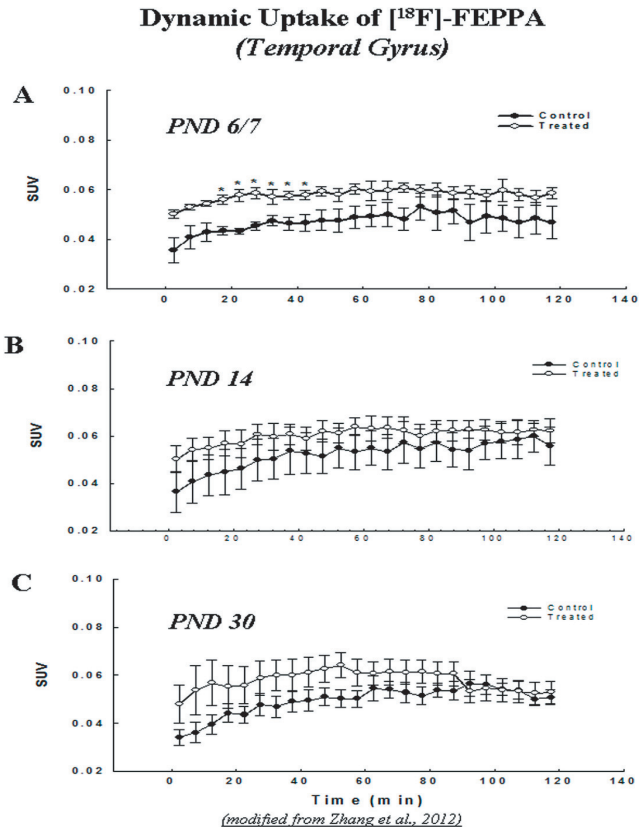

Figure 3: Graph showing the dynamic uptake of [^{18}F]-FEPPA expressed as SUV versus time for the temporal lobe from control and exposed monkeys on PNDs 6 or 7, 14, and 30 ($n = 4$/group). SUV = Standard Uptake Value = average concentration of radioactivity in the ROI (MBq/mL) $\times$ body weight (gram)/injected dose (MBq). Data are shown as the means $\pm$ S.E.M. $^{*}P < .05$.

no significant differences were observed at any time (Figure 3(C)).

At the age of 6 months, the uptake of [^{18}F]-FEPPA in the anesthetic-treated monkeys was similar to that of controls at most of the time points and no significant differences were observed at any time (data not shown).

4 Discussion

A great deal of concern has recently arisen regarding the safety of anesthesia in infants and young children. There is a mounting and convincing preclinical evidence from rodent studies that anesthetics in common clinical use are neurotoxic to the developing brain [10, 13, 24, 38]. Because of obvious limitations, it is not possible to thoroughly explore the effects of pediatric anesthetics on neurons in human infants or children, nor is it possible to determine the dose-response or time-course for potential anesthetic-induced neuronal damage in humans. However, the nonhuman primate provides a closely-related animal model appropriate for examining the effects of pediatric anesthetics and it is in the rhesus monkey that the phenomenon of interest has been previously reported [8, 26, 36, 37]. In addition, the anatomical and functional characterization of the monkey central nervous system (CNS) is extensive, thereby facilitating the interpretation of findings in this animal model. Thus, utilization of the developing nonhuman primate model, when combined with biochemical, pathological, pharmacokinetic, and dynamic molecular imaging approaches, should provide a bridging platform and, thus, serve to provide the most expeditious approaches towards decreasing the uncertainty in extrapolating pre-clinical data to the human condition.

The anesthetic gases N_2O and ISO are commonly used for surgical procedures in human infants. In the present study, the combination of 70% N_2O + 1% ISO in oxygen induced and maintained a steady, light surgical plane of anesthesia in the infant monkey, as evidenced by a lack of voluntary movement, decreased muscle tone, and minimal reaction to physical stimulation with maintenance of an intact palpebral reflex. Neither 70% N_2O nor 1% ISO alone induced or maintained a similar state of anesthesia. It has been reported that N_2O alone at sub-anesthetic concentrations [13, 16] triggers little or no neuroapoptosis, but that it markedly augments isoflurane-induced neuroapoptosis in the developing rat brain. It has also been reported that isoflurane suppresses neurogenesis, which may be linked to widespread neuronal damage [28]. It is clear that the depth of anesthesia achieved with the combination of 70% N_2O and 1% ISO is significantly greater than that achieved with either agent alone at these same concentrations. It is possible that the reduction in neuronal activity associated with deeper levels of anesthesia could by itself trigger neuronal cell death. However, it is of considerable interest that, in the present study, a delivered concentration of 1.0% ISO alone for 8 h did not cause any noticeable increase in abnormal cell death, whereas others have recently demonstrated that exposure to ISO alone at levels resulting in end tidal concentrations of 1.5% for only 5 h is sufficient to significantly increase neuronal and glial apoptosis [3, 20]. This suggests that the threshold concentration of ISO for inducing abnormal apoptosis in primates is likely between 1.0% and 1.5%.

As was the case for the topographic and morphologic expression pattern, statistical analyses of these data indicated that prolonged exposure to the anesthetic combination used in the present study produced a marked increase in the number of neurons which were positive for important histochemical markers such as caspase-3. The caspase-3-positive neurons in these cortical regions still maintained their typical pyramidal morphology and neuronal processes [36]. Although a few isolated caspase-3-positive neuronal cells were observed in some additional

brain areas including the thalamus, striatum, and amygdala, no significant differences were detected between anesthetic combination-treated and control monkeys in these areas for either exposure duration (3 or 8 h). Anesthetic treatment also had no effect on cells in the cerebellum. Previously, electron microscopy data demonstrated typical nuclear condensation, and mitochondrial and nerve cell body swelling in the brains of anesthetic-treated infant monkeys [36]. These data support the hypothesis that anesthetic-induced neuronal cell death in the neonatal monkey is both apoptotic and necrotic in nature. However, electron microscopy and other biochemical and morphological observations in the developing rat have only shown nuclear condensation and fragmentation typical of the advanced stages of apoptosis [38]. Also, previous rodent studies showed that lesions produced by the inhaled anesthetic combination were restricted to the frontal cortex [38]. In contrast to the developing rat, significant increases in neuronal damage were present in multiple brain regions in the developing monkey, particularly in the temporal gyrus, hippocampus and frontal cortex. These observations indicate that the potential toxicological consequences of prolonged anesthetic exposure in primates during development may be far more serious than those produced in rodents.

The high-resolution positron emission tomography scanner (microPET) provides in vivo molecular imaging at a sufficient resolution to resolve both major structures and neuronal activities in the nonhuman primate brain. Since it is known that levels of the peripheral benzodiazepine receptor (PBR), a microglial marker, increase in areas of neuronal injury following exposure to neurotoxicants, the PBR is widely recognized as an important target for imaging via positron emission tomography (PET).

In the CNS, PBRs are mainly located in glial cells, particularly in microglia and astrocytes, with the highest densities in the olfactory bulb, choroid plexus, and ependymal lining of the ventricles [14,11]. In the CNS, PBRs participate in multiple physiological functions including neurosteroid synthesis, nutritional support of neurons and modulation of CNS immune reactions. The expression of the PBR in brain is significantly increased in response to a wide variety of CNS insults. Experimental results show that such increases are mainly due to activated glial cells. In response to intercellular signaling induced by neurotoxicants, microglial activation usually begins several hours after exposure and lasts for several days after the onset of injury [1,12,29]. In their activated state, microglia undergo morphological changes, accumulate and proliferate at the site of neuronal damage, synthesize pro-inflammatory cytokines, and release toxic molecules and metabolites to eliminate damaged cells. Various studies have demonstrated that PBRs are involved in numerous nervous system disorders such as multiple sclerosis, cerebral ischemia and stroke, epilepsy, brain injury, neurotoxic brain damage, and neurodegenerative diseases [2,4,14,19,21].

To determine whether combination inhalation anesthetic exposure during infancy is associated with neurotoxicity, suspected anesthetic-induced neural damage was assessed by monitoring changes in the binding of a peripheral benzodiazepine receptor (PBR) ligand using microPET technology. Since the levels of the PBR increase in areas of neuronal injury following exposure to neurotoxicants, it should be possible in vivo to repeatedly assess anesthetic-induced neuroinflammation that is thought to accompany neurodegeneration by monitoring changes in the uptake of specific radiotracers (e.g., [^{18}F]-FEPPA) that mark glial activation. By employing this non-invasive approach, it is possible to monitor the same subjects repeatedly over extended periods of time, thus, decreasing the need for larger numbers of animals and allowing for animals to serve as their own controls. By utilizing developing nonhuman primates—the most relevant pediatric animal model for studying brain growth, development and function–this study furthers the scientific evaluation of a sensitive population and provides data to directly assess risk in that population. In addition, this study employed a translational biomarker (the PBR ligand [^{18}F]-FEPPA) that should be applicable across species from rodents to humans.

Consistent with the concomitant histochemical findings, the levels of radioactivity in the ROIs were significantly higher in animals exposed to the N_2O/ISO combination. The uptake of [^{18}F]-FEPPA in neocortical areas was higher than in controls at most time points one day after anesthetic treatment and approximately one week after treatment. However, SUVs in both the frontal and temporal cortical areas in treated animals, while higher than those in controls, were not significantly higher on PND 30 or at 6 months of age. These microPET data suggest that developmental exposures to 8 h of a combination of N_2O and ISO result in neuronal damage that is reflected by an increase in glial activation, as evidenced by an increased presence of PBRs, markers of glial activation thought to accompany adverse events such as neuronal damage and death. [^{18}F]-FEPPA, as a marker of gliosis, may be useful for indicating the location of distressed neurons. It is proposed that PET imaging using this biomarker will help detect neurotoxicity in a variety of species including humans. By repeatedly assessing the concentration of labeled FEPPA in affected areas [34,35] it should be possible to evaluate the severity, time course, and location of anesthetic-induced neuronal damage in living animals. The use of the developing monkey would seem to provide an excellent bridging platform to aid in the translation of findings from lower species to higher species and, thus, serve to provide the most expeditious approach towards decreasing the uncertainty in extrapolating pre-clinical data to the human condition.

There are yet many questions that need to be answered before the findings of anesthetic-induced neurotoxicity observed in animals can be related to clinical situations. However, it is hoped that molecular imaging using radiolabeled biomarkers will help detect and monitor neurotoxicity across a wide range of ages and exposure situations in multiple species including humans. The use of a nonhuman primate model combined with appropriate molecular imaging tools may well be one of the most practical approaches for evaluating the location, time course, and severity of neuronal damage associated with anesthetic or sedative exposures during development.

Acknowledgments This work was supported by the National Center for Toxicological Research (NCTR)/U.S. Food and Drug Administration (FDA), the Center for Drug Evaluation and Research (CDER)/FDA, and the National Institute of Child Health and Human Development (NICHD).

Disclaimer This document has been reviewed in accordance with United States Food and Drug Administration (FDA) policy and approved for publication. Approval does not signify that the contents necessarily reflect the position or opinions of the FDA. The findings and conclusions in this report are those of the authors and do not necessarily represent the views of the FDA.

References

[1] R. B. Banati, *Neuropathological imaging: in vivo detection of glial activation as a measure of disease and adaptive change in the brain*, Br Med Bull, 65 (2003), 121–131.

[2] J. Benavides, D. Fage, C. Carter, and B. Scatton, *Peripheral type benzodiazepine binding sites are a sensitive indirect index of neuronal damage*, Brain Res, 421 (1987), 167–172.

[3] A. Brambrink, A. Evers, M. Avidan, N. Farber, D. Smith, X. Zhang, et al., *Isoflurane-induced neuroapoptosis in the neonatal rhesus macaque brain*, Anesthesiology, 112 (2010), 834–841.

[4] E. Briard, S. S. Zoghbi, M. Imaizumi, J. P. Gourley, H. U. Shetty, J. Hong, et al., *Synthesis and evaluation in monkey of two sensitive ^{11}C-labeled aryloxyanilide ligands for imaging brain peripheral benzodiazepine receptors in vivo*, J Med Chem, 51 (2008), 17–30.

[5] A. F. Chatziioannou, *Molecular imaging of small animals with dedicated PET tomographs*, Eur J Nucl Med Mol Imaging, 29 (2002), 98–114.

[6] K. Dikranian, Y. Q. Qin, J. Labruyere, B. Nemmers, and J. W. Olney, *Ethanol-induced neuroapoptosis in the developing rodent cerebellum and related brain stem structures*, Brain Res Dev Brain Res, 155 (2005), 1–13.

[7] K. A. Haberny, M. G. Paule, A. C. Scallet, F. D. Sistare, D. S. Lester, J. P. Hanig, et al., *Ontogeny of the N-methyl-D-aspartate (NMDA) receptor system and susceptibility to neurotoxicity*, Toxicol Sci, 68 (2002), 9–17.

[8] C. E. Hotchkiss, C. Wang, and W. Slikker Jr., *Effect of prolonged ketamine exposure on cardiovascular physiology in pregnant and infant rhesus monkeys (Macaca mulatta)*, J Am Assoc Lab Anim Sci, 46 (2007), 21–28.

[9] C. Ikonomidou, P. Bittigau, M. Ishimaru, D. Wozniak, C. Koch, K. Genz, et al., *Ethanol-induced apoptotic neurodegeneration and fetal alcohol syndrome*, Science, 287 (2000), 1056–1060.

[10] C. Ikonomidou, F. Bosch, M. Miksa, P. Bittigau, J. Vöckler, K. Dikranian, et al., *Blockade of NMDA receptors and apoptotic neurodegeneration in the developing brain*, Science, 283 (1999), 70–74.

[11] M. Imaizumi, E. Briard, S. S. Zoghbi, J. P. Gourley, J. Hong, Y. Fujimura, et al., *Brain and whole-body imaging in nonhuman primates of [^{11}C]PBR28, a promising PET radioligand for peripheral benzodiazepine receptors*, Neuroimage, 39 (2008), 1289–1298.

[12] F. Ito, H. Toyama, G. Kudo, H. Suzuki, K. Hatano, M. Ichise, et al., *Two activated stages of microglia and PET imaging of peripheral benzodiazepine receptors with [^{11}C]PK11195 in rats*, Ann Nucl Med, 24 (2010), 163–169.

[13] V. Jevtovic-Todorovic, R. E. Hartman, Y. Izumi, N. D. Benshoff, K. Dikranian, C. F. Zorumski, et al., *Early exposure to common anesthetic agents causes widespread neurodegeneration in the developing rat brain and persistent learning deficits*, J Neurosci, 23 (2003), 876–882.

[14] S. Lang, *The role of peripheral benzodiazepine receptors (PBRs) in CNS pathophysiology*, Curr Med Chem, 9 (2002), 1411–1415.

[15] G. D. Luker, V. Sharma, and D. Piwnica-Worms, *Visualizing protein-protein interactions in living animals*, Methods, 29 (2003), 110–122.

[16] D. Ma, P. Williamson, A. Januszewski, M. C. Nogaro, M. Hossain, L. P. Ong, et al., *Xenon mitigates isoflurane-induced neuronal apoptosis in the developing rodent brain*, Anesthesiology, 106 (2007), 746–753.

[17] R. Myers, *The biological application of small animal PET imaging*, Nucl Med Biol, 28 (2001), 585–593.

[18] J. V. Nadler and D. A. Evenson, *Use of excitatory amino acids to make axon-sparing lesions of hypothalamus*, Methods Enzymol, 103 (1983), 393–400.

[19] N. Oku, T. Kashiwagi, and J. Hatazawa, *Nuclear neuroimaging in acute and subacute ischemic stroke*, Ann Nucl Med, 24 (2010), 629–638.

[20] J. Olney, A. M. Brambrink, M. S. Avidan, N. B. Farber, and S. A. Back, *Isoflurane-induced oligoapoptosis in neonatal rhesus macaque brain*. American Society of Anesthesiologists Annual Meeting, 2010.

[21] V. Papadopoulos, L. Lecanu, R. C. Brown, Z. Han, and Z. X. Yao, *Peripheral-type benzodiazepine receptor in neurosteroid biosynthesis, neuropathology and neurological disorders*, Neuroscience, 138 (2006), 749–756.

[22] G. Paxinos, X. F. Huang, and A. W. Toga, *The Rhesus Monkey Brain in Stereotaxic Coordinates*, Academic Press, San Diego, 2000.

[23] M. E. Phelps, *Positron emission tomography provides molecular imaging of biological processes*, Proc Natl Acad Sci U S A, 97 (2000), 9226–9233.

[24] A. C. Scallet, L. C. Schmued, W. Slikker Jr., N. Grunberg, P. J. Faustino, H. Davis, et al., *Developmental neurotoxicity of ketamine: morphometric confirmation, exposure parameters, and multiple fluorescent labeling of apoptotic neurons*, Toxicol Sci, 81 (2004), 364–370.

[25] L. C. Schmued, C. C. Stowers, A. C. Scallet, and L. Xu, *Fluoro-Jade C results in ultra high resolution and contrast labeling of degenerating neurons*, Brain Res, 1035 (2005), 24–31.

[26] W. Slikker Jr., X. Zou, C. Hotchkiss, R. Divine, N. Sadovova, N. Twaddle, et al., *Ketamine-induced neuronal cell death in the perinatal rhesus monkey*, Toxicol Sci, 98 (2007), 145–158.

[27] L. A. Sternberger, P. H. Hardy Jr., J. J. Cuculis, and H. G. Meyer, *The unlabeled antibody enzyme method of immunohistochemistry: preparation and properties of soluble antigen-antibody complex (horseradish peroxidase-antihorseradish peroxidase) and its use in identification of spirochetes*, J Histochem Cytochem, 18 (1970), 315–333.

[28] G. Stratmann, K. Visrodia, L. May, J. Sall, and Y. Shin, *Effects of isoflurane on hippocampal neurogenesis in neonatal rats*. American Society of Anesthesiologists Annual Meeting, 2009.

[29] A. Takeuchi, K. I. Isobe, O. Miyaishi, M. Sawada, Z. H. Fan, I. Nakashima, et al., *Microglial NO induces delayed neuronal death following acute injury in the striatum*, Eur J Neurosci, 10 (1998), 1613–1620.

[30] C. Wang, N. Sadovova, X. Fu, L. Schmued, A. Scallet, J. Hanig, et al., *The role of the N-methyl-D-aspartate receptor in ketamine-induced apoptosis in rat forebrain culture*, Neuroscience, 132 (2005), 967–977.

[31] C. Wang, N. Sadovova, C. Hotchkiss, X. Fu, A. C. Scallet, T. A. Patterson, et al., *Blockade of N-methyl-D-aspartate receptors by ketamine produces loss of postnatal day 3 monkey frontal cortical neurons in culture*, Toxicol Sci, 91 (2006), 192–201.

[32] C. Young, B. J. Klocke, T. Tenkova, J. Choi, J. Labruyere, Y. Q. Qin, et al., *Ethanol-induced neuronal apoptosis in vivo requires BAX in the developing mouse brain*, Cell Death Differ, 10 (2003), 1148–1155.

[33] C. Young, K. A. Roth, B. J. Klocke, T. West, D. M. Holtzman, J. Labruyere, et al., *Role of caspase-3 in ethanol-induced developmental neurodegeneration*, Neurobiol Dis, 20 (2005), 608–614.

[34] X. Zhang, M. G. Paule, G. D. Newport, N. Sadovova, M. S. Berridge, S. M. Apana, et al., *MicroPET imaging of ketamine-induced neuronal apoptosis with radiolabeled DFNSH*, J Neural Transm, 118 (2011), 203–211.

[35] X. Zhang, M. G. Paule, G. D. Newport, X. Zou, N. Sadovova, M. S. Berridge, et al., *A minimally invasive, translational biomarker of ketamine-induced neuronal death in rats: microPET imaging using ^{18}F-annexin V*, Toxicol Sci, 111 (2009), 355–361.

[36] X. Zou, F. Liu, X. Zhang, T. A. Patterson, R. Callicott, S. Liu, et al., *Inhalation anesthetic-induced neuronal damage in the developing rhesus monkey*, Neurotoxicol Teratol, 33 (2011), 592–597.

[37] X. Zou, T. A. Patterson, R. L. Divine, N. Sadovova, X. Zhang, J. P. Hanig, et al., *Prolonged exposure to ketamine increases neurodegeneration in the developing monkey brain*, Int J Dev Neurosci, 27 (2009), 727–731.

[38] X. Zou, N. Sadovova, T. A. Patterson, R. L. Divine, C. E. Hotchkiss, S. F. Ali, et al., *The effects of L-carnitine on the combination of, inhalation anesthetic-induced developmental, neuronal apoptosis in the rat frontal cortex*, Neuroscience, 151 (2008), 1053–1065.